An Adjustable Uncertainty Set Constrained Unit Commitment with Operation Risk Reduced through Demand Response

Y. F. Du, Y. Z. Li, C. Duan, H. B. Gooi, *Senior Member, IEEE,* and L. Jiang

***Abstract*—In this paper, the approach of an adjustable uncertainty set is proposed to deal with the uncertainty of renewable energy (RE) in unit commitment (UC). Demand response (DR) is co-optimized to reduce the operation risk of load shedding and RE curtailment when the RE falls out of the adjustable uncertainty set. In comparison with existing approaches with an adjustable uncertainty set, the proposed approach further incorporates DR and it requires no predefined parameters to constrain the deviation from the forecast RE. It divides the maximum RE set into subintervals, and bounds of the adjustable uncertainty set are determined among these subintervals with the consideration of DR in reducing the operation risk. The original mixed integer nonlinear problem of UC scheduling is transformed to be a mixed integer linear problem to be effectively solved. The performance of the proposed approach is verified on the IEEE 6-bus, 30-bus and 300-bus systems. Through the comparison with existing methods, the effectiveness of the proposed approach in reducing the conservativeness is verified. The effectiveness of the proposed approach in the reduction of the operation risk of load shedding and RE curtailment is verified through the comparison between situations with and without DR.**

***Index Terms*—Adjustable uncertainty set, demand response, unit commitment, renewable energy**

NOMENCLATURE

Abbreviation

RE	Renewable energy.
UC	Unit commitment.
SOA	Stochastic optimization approach.
ROA	Robust optimization approach.
DROA	Distributionally robust optimization approach.
DR	Demand response.
MILP	Mixed integer linear programming.

Parameters

$\mathcal{B}$	Set of all buses.
$\mathcal{L}$	Set of all lines.
$\mathcal{T}$	Set of all time slots.
$\mathcal{G}_b$	Set of all units at bus b.
SU_i^b	Start-up cost of unit i at bus b.
SD_i^b	Shut-down cost of unit i at bus b.
$f_{i,0}^{jb}$,$f_{i,1}^{jb}$	jth piecewise cost coefficients of unit i at bus b.
C_{ls}	Penalty price of load shedding.
C_{rc}	Penalty price of RE curtailment.
R_{ld}	Incentive price for load decrease in DR.
R_{li}	Incentive price for load increase in DR.
T	UC scheduling horizon.
MU_i^b	Minimum up-time of unit i at bus b.
MD_i^b	Minimum down-time of unit i at bus b.
IC_i^b	Minimum time of unit i at bus b in the initial on/off state.
UR_i^b	Ramp-up rate limit of unit i at bus b.
DR_i^b	Ramp-down rate limit of unit i at bus b.
$\overline{UR}_i^b$	First-hour minimum output power of unit i at bus b.
$\overline{DR}_i^b$	Last-hour minimum output power of unit i at bus b.
$\overline{LR}_{\max}^b$	Maximum load increase of DR at bus b.
$\underline{LR}_{\max}^b$	Maximum load decrease of DR at bus b.
LB_t^b	Lower bound of output power of RE at bus b in time t.
UB_t^b	Upper bound of output power of RE at bus b in time t.
$\overline{\Delta}_t^b$	Positive deviation unit of RE at bus b in time t.
$\underline{\Delta}_t^b$	Negative deviation unit of RE at bus b in time t.
N	Division number of RE.
L_i^b	Lower bound of output power of unit i at bus b.
U_i^b	Upper bound of output power of unit i at bus b.
C_l	Capacity of transmission line l.
K_l^b	Load shift factor from bus b to line l.
β_b	Capacity of load change of DR at bus b.
w_t^b	Actual output power of RE at bus b in time t.
$\hat{w}_t^b$	Forecast output power of RE at bus b in time t.
$\hat{\xi}_t^b$	Forecast load at bus b in time t.

Y. F. Du is with the School of Mechanical and Electrical Engineering, University of Electronic Science and Technology of China, Chengdu 611731, China.

Y. Z. Li is with the School of Artificial Intelligence and Automation, Huazhong University of Science and Technology, Wuhan 430074, China, and also with Key Laboratory of Control of Power Transmission and Conversion (SJTU), Ministry of Education, Shanghai 200240. (e-mail: Yuanzheng_Li@hust.edu.cn).

C. Duan is with the Department of Physics and Astronomy, Northwestern University, Evanston, U.S..

H. B. Gooi is with the School of Electrical and Electronic Engineering, Nanyang Technological University, Singapore 639798.

L. Jiang is with the Department of Electrical Engineering and Electronics, The University of Liverpool, Liverpool L69 3GJ, U.K..

The work is supported in part by the Key Scientific and Technological Research Project of State Grid Corporation of China-Research on the Mechanism of Internet of Thing and its Key Supporting Technologies for Smooth Integration, in part by National Natural Science Foundation of China (Grant No. 51707069), in part by Key Laboratory of Control of Power Transmission and Conversion (SJTU), Ministry of Education (2018AB03), and in part by the Fundamental Research Funds for the Central Universities (Grant No. 2019kfy-XJJS17). (Corresponding author: Yuanzheng Li.)

α Proportion of DR failure.
λ Weight factor between the operation cost of UC and the operation risk of load shedding and RE curtailment.
$\overline{\gamma}^b$ Limit of positive deviation number of RE at bus b in the scheduling horizon.
$\underline{\gamma}^b$ Limit of negative deviation number of RE at bus b in the scheduling horizon.

Decision variables

$Risk_t^b$ Without DR failure, maximum risk of load shedding and RE curtailment at bus b in time t.
$URisk_t^b$ Additional risk of load shedding and RE curtailment at bus b in time t due to DR failure.
$\overline{LR}_t^b$ Load increase of DR at bus b in time t.
$\underline{LR}_t^b$ Load decrease of DR at bus b in time t.
LB'^b_t Adjusted lower bound of output power of RE at bus b in time t.
UB'^b_t Adjusted upper bound of output power of RE at bus b in time t.
$\overline{Q}_t^b$ Positive deviation number of RE at bus b in time t.
$\underline{Q}_t^b$ Negative deviation number of RE at bus b in time t.
y_{it}^b Binary decision variable: "1" if unit i at bus b is on in time t; "0" otherwise.
u_{it}^b Binary decision variable: "1" if unit i at bus b is started up in time t; "0" otherwise.
v_{it}^b Binary decision variable: "1" if unit i at bus b is shut down in time t; "0" otherwise.
x_{it}^b Output power schedule of unit i at bus b in time t.
a_{it}^b Participation factor of unit i at bus b in time t.
$\underline{q}_{tn}^b, \underline{h}_{rtn}^b$ Auxiliary variables.
$\overline{Q}_t^b, H_{rt}^b$ Auxiliary variables.

I. Introduction

CURRENTLY, renewable energy (RE) is largely integrated in power systems due to increasing concerns on a clean environment and reduction of green-house gases. The capacity of RE excluding hydroelectric energy accounted for 10.3% of the global power generation and took up 53.6% of the global capacity of newly installed power generators in 2015 [1]. However, its intermittency and uncertainty brings a great challenge to the power system operation including unit commitment (UC) [2].

Various methods have been proposed to deal with the uncertainty of RE in UC. The most commonly used methods are stochastic optimization approach (SOA) and robust optimization approach (ROA). The SOA usually requires a large number of scenarios which are generated from an exact probability distribution of RE. For instance, Ref. [3] considers scenarios of RE and minimizes the expected operation cost through the SOA. On the contrary, the ROA does not require the exact probability distribution of RE. Ref. [4] adopts the maximum uncertainty set and minimizes the operation cost under the worst-case scenario of RE through the ROA. However, this approach is conservative since it takes into account the worst case. With the combination of SOA and ROA, distributionally robust optimization approach (DROA) is proposed to deal with the uncertainty of RE recently. Ref. [5] extracts probabilistic information from historical data and takes into account the probabilistic information to construct an ambiguity set of probability distribution of RE. Then it considers the worst probability distribution of RE based on the DROA and minimizes the operation cost of UC. The DROA does not require the exact probability distribution of RE in comparison with the SOA and it is less conservative than the ROA since some probabilistic information is used.

In recent years, the approach of an adjustable uncertainty set has been proposed to tackle the uncertainty of RE. Ref. [6] and Ref. [7] determine an adjustable uncertainty set of RE with predefined parameters to limit the number of deviation from the forecast RE. In the adjustable uncertainty set, a feasible solution of UC certainly exists without load shedding and RE curtailment. To determine the adjustable uncertainty set, Ref. [8] divides the maximum uncertainty set into subsets and predefines parameters to constrain the deviation number from the forecast RE when UC is scheduled. In comparison with SOA and DROA, the approach of an adjustable uncertainty set determines a subset within the maximum uncertainty set and can guarantee a feasible solution in this subset. It is less conservative than the ROA since it narrows the uncertainty set of RE which is taken into account in UC. However, the predefined parameters which constrain deviation are required when the adjustable uncertainty set is determined [6]–[8].

Demand response (DR) has been taken into account to deal with the uncertainty of RE for its response to the variation of RE. DR participates in tackling the uncertainty of RE either as energy or reserve resources. Ref. [9] schedules the energy of DR and the output power of generators in UC with the uncertainty of RE. With the help of flexibilities of DR, substantial benefits in terms of redispatch costs can be achieved. In Ref. [10], the system operator accepts reserve offers from both generators and DR, which is shown to be effective to host high penetration of RE.

This paper combines adjustable uncertainty set and DR to tackle the uncertainty of RE in UC, and it improves the existing approaches of an adjustable uncertainty set. Within the adjustable uncertainty set, the proposed approach guarantees a solution of UC without load shedding and RE curtailment. When RE falls out of the adjustable uncertainty set, there exists the operation risk of load shedding and RE curtailment. DR is adopted as reserve resources to reduce this operation risk. In comparison with the existing approaches with adjustable uncertainty set [6]–[8], the proposed approach does not require predefined parameters to constrain the deviation from the forecast RE. Firstly, the maximum uncertainty set of RE is divided into subintervals in the proposed approach. Without predefined parameters, bounds of the adjustable uncertainty set are determined among subintervals by considering the operation risk of load shedding and RE curtailment and the participation of DR in reducing the operation risk. In comparison with the existing methods in which DR is treated as reserve resources, the participation of DR is conditional and

will be taken in when RE is out of the adjustable uncertainty set. With the approval of consumers, DR decreases the load consumption when RE is less than the lower bound of the adjustable uncertainty set and increases the load consumption when RE exceeds the upper bound. The contributions of this paper are summarized as follows,

- This paper combines the adjustable uncertainty set and DR to tackle the uncertainty of RE. The adjustable uncertainty set and DR are individually adopted in existing references. With the adjustable uncertainty set, the conservativeness of the proposed approach is reduced in comparison with ROA since the adjustable uncertainty set is a subset of the maximum uncertainty set. However, the adjustable uncertainty set brings about the operation risk of load shedding and RE curtailment. Together with the participation of DR, the operation risk is reduced in the proposed approach.
- The proposed approach of an adjustable uncertainty set improves the existing approaches of an adjustable uncertainty set and it does not require predefined parameters to limit the deviation from the forecast RE. The existing methods require predefined parameters to determine the adjustable uncertainty set while the proposed method does not require these parameters. With the maximum uncertainty set of RE divided into subintervals, the proposed approach determines bounds of the adjustable uncertainty set among these subintervals without predefined parameters.
- The original mixed integer nonlinear problem of UC scheduling is reformulated into a tractable mixed integer linear problem for which efficient solvers are available. Based on the proposed approach, the counterpart of adjustable uncertainty set will involve the product of continuous decision variables and integer decision variables that indicate which subinterval is adopted as the adjustable uncertainty set. Sums of binary variables are introduced to replace the integer decision variables, which transforms the product of integer and continuous variables to be the product of binary and continuous variables. With extra linear constraints introduced to replace the product of binary and continuous variables, the UC scheduling is solved effectively by mixed integer linear programming (MILP).

The effectiveness of the proposed approach in scheduling UC with the consideration of the uncertainty of RE and applying DR to the reduction of operation risk is tested on IEEE 6-bus, 30-bus and 300-bus systems. Through comparisons with the ROA and a method that constrains the deviation from the forecast RE, the effectiveness of the proposed approach on reducing the conservativeness is tested. The effect of DR on reducing the operation risk of load shedding and RE curtailment is investigated through the comparison of situations with and without DR.

The rest of this paper is organized as follows. The problem formulation of UC based on the proposed approach is presented in Section II. Section III proposes the solution approach to reformulate the original problem to be linear to be solved by MILP. Simulation results are presented in Section IV and conclusions are given in Section V.

II. Problem Formulation

In this section, firstly the UC problem with the traditional ROA is shown. Then, the approach with an adjustable uncertainty set and DR is proposed, and the corresponding formulation of the UC problem via the proposed approach is presented.

A. Unit commitment via the robust optimization approach

The UC problem is usually modelled based on the affinely adjustable approach [11] or the two-stage adaptive approach. The affinely adjustable approach is adopted in this paper since it is more computationally tractable [5]. In the affinely adjustable approach, the actual power outputs of units p_{it}^b are adjusted to compensate the forecast error of RE, which is formulated as follows,

$$p_{it}^b = x_{it}^b + a_{it}^b \sum_{b\in\mathcal{B}} (\hat{w_t^b} - w_t^b), \tag{1}$$

where x_{it}^b represents the output power schedule of unit i at bus b in time t. When the actual output power of RE w_t^b deviates from the forecast RE $\hat{w_t^b}$, the actual output power of unit is adjusted according to a proportion a_{it}^b of the forecast error of RE. By taking into account the uncertainty of RE via the ROA, the problem of UC based on the affinely adjustable approach is formulated as follows,

$$\min_{\boldsymbol{u},\boldsymbol{v},\boldsymbol{y},\boldsymbol{x},\boldsymbol{a}} \left\{ \sum_{t\in\mathcal{T}} \sum_{b\in\mathcal{B}} \sum_{i\in\mathcal{G}_b} SU_i^b u_{it}^b + SD_i^b v_{it}^b + F_i^b(y_{it}^b, x_{it}^b) \right\} \tag{2a}$$

$$s.t.\ \forall i \in \mathcal{G}_b, \forall b \in \mathcal{B}, \forall l \in \mathcal{L}, \forall t \in \mathcal{T}$$

$$p_{it}^b = x_{it}^b + a_{it}^b \sum_{b\in\mathcal{B}} (\hat{w_t^b} - w_t^b) \tag{2b}$$

$$\begin{aligned} &-y_{i(t-1)}^b + y_{it}^b - y_{ik}^b \le 0 \\ &\forall k \in [t+1, \min\{t + MU_i^b - 1, T\}] \end{aligned} \tag{2c}$$

$$\begin{aligned} &y_{i(t-1)}^b - y_{it}^b + y_{ik}^b \le 1 \\ &\forall k \in [t+1, \min\{t + MD_i^b - 1, T\}] \end{aligned} \tag{2d}$$

$$y_{it}^b = y_{i1}^b, t \in [1, IC_i^b] \tag{2e}$$

$$-y_{i(t-1)}^b + y_{it}^b - u_{it}^b \le 0 \tag{2f}$$

$$y_{i(t-1)}^b - y_{it}^b - v_{it}^b \le 0 \tag{2g}$$

$$y_{it}^b, u_{it}^b, v_{it}^b \in \{0, 1\} \tag{2h}$$

$$0 \le a_{it}^b \le y_{it}^b \tag{2i}$$

$$\sum_{b\in\mathcal{B}} \sum_{i\in\mathcal{G}_b} (x_{it}^b - a_{it}^b \sum_{b\in\mathcal{B}} (\hat{\xi_t^b} - \hat{w_t^b})) = 0 \tag{2j}$$

$$\sum_{b\in\mathcal{B}} \sum_{i\in\mathcal{G}_b} a_{it}^b = 1 \tag{2k}$$

$$\begin{aligned} &p_{it}^b - p_{i(t-1)}^b \le (2 - y_{i(t-1)}^b - y_{it}^b)\overline{UR}_i^b \\ &+ (1 + y_{i(t-1)}^b - y_{it}^b) UR_i^b,\ \forall w_t^b \in [LB_t^b, UB_t^b] \\ &p_{i(t-1)}^b - p_{it}^b \le (2 - y_{i(t-1)}^b - y_{it}^b)\overline{DR}_i^b \end{aligned} \tag{2l}$$

$$+(1-y^b_{i(t-1)}+y^b_{it})DR^b_i,\ \forall w^b_t\in[LB^b_t,UB^b_t] \tag{2m}$$

$$p^b_{it}-L^b_i y^b_{it}\geq 0,\ \forall w^b_t\in[LB^b_t,UB^b_t] \tag{2n}$$

$$p^b_{it}-U^b_i y^b_{it}\leq 0,\ \forall w^b_t\in[LB^b_t,UB^b_t] \tag{2o}$$

$$\sum_{b\in\mathcal{B}}K^b_l(\sum_{r\in\mathcal{G}_b}p^b_{rt}-(\hat{\xi^b_t}-w^b_t))+C_l\geq 0,\ \forall w^b_t\in[LB^b_t,UB^b_t] \tag{2p}$$

$$\sum_{b\in\mathcal{B}}K^b_l(\sum_{r\in\mathcal{G}_b}p^b_{rt}-(\hat{\xi^b_t}-w^b_t))-C_l\leq 0,\ \forall w^b_t\in[LB^b_t,UB^b_t] \tag{2q}$$

where $F^b_i(y^b_{it},x^b_{it})\geq f^{jb}_{i,0}y^b_{it}+f^{jb}_{i,1}x^b_{it},\ \forall t\in\mathcal{T},b\in\mathcal{B},i\in\mathcal{G}_b,j=1,2,3$, and the generation cost function of units $F^b_i(y^b_{it},x^b_{it})$ is expressed as a piecewise linear function. The generation cost function of units is usually calculated as a quadratic function and three linear functions are adopted to linearize the quadratic function, i.e., $f^{jb}_{i,0}y^b_{it}+f^{jb}_{i,1}x^b_{it}, j=1,2,3$. The uncertainty of RE is taken into account via the ROA in constraints (2l)-(2q) and these constraints are required to be satisfied under all scenarios of RE within the maximum uncertainty set, i.e., $[LB^b_t,UB^b_t]$. Constraints (2c) and (2d) represent the restrictions for the minimum up-time and down-time of units, respectively. For example, if $y^b_{i(t-1)}=0$ and $y^b_{it}=1$, which shows that the unit is started at time slot t. According to (2c), $y^b_{ik}=1,\forall k\in[t+1,\min\{t+MU^b_i-1,T\}]$ since the unit is required to be on for minimum up-time MU^b_i from the time slot when it is started. Constraint (2e) represents the minimum time for which units should stay in the initial on/off states due to the minimum up/down-time of units confined in the previous scheduling horizon. Constraints (2f) and (2g) indicate the start-up and the shut-down of units. For example, if $y^b_{i(t-1)}=0$ and $y^b_{it}=1$, which shows that the unit is started at time slot t, and according to (2f), $u^b_{it}=1$. Constraint (2i) enforces limits on the participation factor of each unit. (2j) and (2k) indicate the balance between generation and load. Constraint (2l) requires the first-hour minimum generation, i.e., $\overline{UR}^b_i$, and the ramp-up rate limit. For example, if $y^b_{i(t-1)}=0$ and $y^b_{it}=1$, (2l) indicates $p^b_{it}-p^b_{i(t-1)}\leq\overline{UR}^b_i$; if $y^b_{i(t-1)}=y^b_{it}=1$, (2l) indicates $p^b_{it}-p^b_{i(t-1)}\leq UR^b_i$. Similarly, constraint (2m) requires the last-hour minimum generation, i.e., $\overline{DR}^b_i$, and the ramp-down rate limit. Constraints (2n) and (2o) ensure that each unit's actual output power is within limits. Constraints (2p) and (2q) represent capacity limits of transmission lines.

B. Improvement via the proposed approach

Since the ROA considers the worst-case scenario within the maximum uncertainty set of RE, it is conservative. The approach of an adjustable uncertainty set is proposed to reduce the conservativeness of the ROA. When the RE falls out of the adjustable uncertainty set, the operation risk of load shedding and RE curtailment is reduced through the participation of DR. The adjustable uncertainty set, the participation of DR and the complete problem formulation of UC based on the proposed approach are introduced in the following subsections.

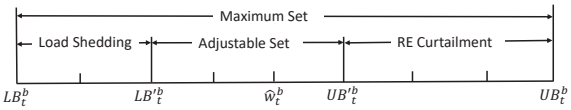

Fig. 1. Adjustable uncertainty set

1) Adjustable uncertainty set: As shown in Fig. 1, $\hat{w^b_t}$ indicates the forecast RE. The output power of RE is within a maximum uncertainty set $[LB^b_t, UB^b_t]$ [5] [7], i.e. LB^b_t and UB^b_t represent the lower and upper bounds of the power output of RE, respectively. In order to reduce the conservativeness of the ROA, the adjustable uncertainty set is introduced with variables indicating the level of deviation from the forecast RE. The adjustable uncertainty set is formulated as follows,

$$LB'^b_t=\hat{w^b_t}-\underline{Q}^b_t\cdot\underline{\Delta}^b_t \tag{3a}$$

$$UB'^b_t=\hat{w^b_t}+\overline{Q}^b_t\cdot\overline{\Delta}^b_t \tag{3b}$$

$$\underline{\Delta}^b_t=\frac{\hat{w^b_t}-LB^b_t}{N} \tag{3c}$$

$$\overline{\Delta}^b_t=\frac{UB^b_t-\hat{w^b_t}}{N} \tag{3d}$$

where (3c) and (3d) show that the maximum positive and negative deviations from the forecast RE are divided into N subintervals. $0\leq\underline{Q}^b_t,\overline{Q}^b_t\leq N$ in (3a) and (3b) are integer variables and indicate levels of negative and positive deviations from the forecast RE, respectively. Note that $\underline{Q}^b_t$ and $\overline{Q}^b_t$ are decision variables and no presumed values are given to them. LB'^b_t and UB'^b_t represent the lower and upper bounds of the adjustable uncertainty set, respectively. It is proposed that (2l)-(2q) are satisfied within $[LB'^b_t,UB'^b_t]$, which are presented as

$$p^b_{it}-p^b_{i(t-1)}\leq(2-y^b_{i(t-1)}-y^b_{it})\overline{UR}^b_i+(1+y^b_{i(t-1)}-y^b_{it})UR^b_i,\ \forall w^b_t\in[LB'^b_t,UB'^b_t] \tag{4a}$$

$$p^b_{i(t-1)}-p^b_{it}\leq(2-y^b_{i(t-1)}-y^b_{it})\overline{DR}^b_i+(1-y^b_{i(t-1)}+y^b_{it})DR^b_i,\ \forall w^b_t\in[LB'^b_t,UB'^b_t] \tag{4b}$$

$$p^b_{it}-L^b_i y^b_{it}\geq 0,\ \forall w^b_t\in[LB'^b_t,UB'^b_t] \tag{4c}$$

$$p^b_{it}-U^b_i y^b_{it}\leq 0,\ \forall w^b_t\in[LB'^b_t,UB'^b_t] \tag{4d}$$

$$\sum_{b\in\mathcal{B}}K^b_l(\sum_{r\in\mathcal{G}_b}p^b_{rt}-(\hat{\xi^b_t}-w^b_t))+C_l\geq 0,\ \forall w^b_t\in[LB'^b_t,UB'^b_t] \tag{4e}$$

$$\sum_{b\in\mathcal{B}}K^b_l(\sum_{r\in\mathcal{G}_b}p^b_{rt}-(\hat{\xi^b_t}-w^b_t))-C_l\leq 0,\ \forall w^b_t\in[LB'^b_t,UB'^b_t]. \tag{4f}$$

Compared with the ROA which requires (2l)-(2q) are satisfied in the maximum uncertainty set of RE, the proposed approach of an adjustable uncertainty set only requires they are satisfied in the subset of the maximum uncertainty set, which makes the proposed approach less conservative than the ROA.

Fig. 2. Demand response for reducing the operation risk

2) Participation of demand response: When an adjustable uncertainty set is considered, the operation risk of load shedding and RE curtailment arises when the RE falls into the maximum uncertainty set excluding the adjustable set. DR can help reduce this risk.

The operation risk under the situation without DR is shown in Fig. 1. There exist risks of load shedding and RE curtailment when the RE is within the interval $[LB_t^b, LB'^b_t]$ and $[UB'^b_t, UB_t^b]$, respectively. Without the participation of DR, the maximum operation risk is formulated as follows,

$$Risk_t^b \geq C_{ls} \cdot (LB'^b_t - LB_t^b) \tag{5a}$$
$$Risk_t^b \geq C_{rc} \cdot (UB_t^b - UB'^b_t), \tag{5b}$$

where $Risk_t^b$ takes bigger value of operation risks of load shedding and RE curtailment. Fig. 2 shows the operation risk under the situation with DR. As shown in Fig. 2, DR can decrease the energy consumption to reduce the risk of load shedding or increase the energy consumption to reduce the risk of RE curtailment. With agreement of consumers, incentive payment will be paid based on load decrease and increase consumers can provide. Note that the load decrease in DR is different from load shedding. DR is based on the flexibility of demand and it is with approval and agreement with consumers [12], while load shedding indicates load cut off under urgent situations where the operational safety of power systems is threatened [6] and it is without consumers' agreement. After DR is taken into account, the maximum operation risk is formulated as follows,

$$Risk_t^b \geq C_{ls} \cdot (LB'^b_t - (LB_t^b + \underline{LR}_t^b)) \tag{6a}$$
$$Risk_t^b \geq C_{rc} \cdot ((UB_t^b - \overline{LR}_t^b) - UB'^b_t). \tag{6b}$$

The amount of load change in DR in each time slot and whole time horizon should be within the following limits [13],

$$0 \leq \underline{LR}_t^b \leq \underline{LR}_{\max}^b \tag{7a}$$
$$0 \leq \overline{LR}_t^b \leq \overline{LR}_{\max}^b \tag{7b}$$
$$\sum_{t\in\mathcal{T}} \underline{LR}_t^b \leq \beta_b \tag{7c}$$
$$\sum_{t\in\mathcal{T}} \overline{LR}_t^b \leq \beta_b \tag{7d}$$

where (7a) and (7b) indicate that DR satisfies power limits while (7c) and (7d) indicate that DR satisfies the capacity limits. To motivate consumers to participate in DR, they will get the incentive payment as $\sum_{t\in\mathcal{T}} R_{ld} \cdot \underline{LR}_t^b + R_{li} \cdot \overline{LR}_t^b$ [14] [15].

With the consideration of the uncertainty of consumers' participation in DR program, for example, communication failures and cyber-attacks, the operation risk of load shedding and RE curtailment is increased by

$$URisk_t^b = \alpha \cdot MRisk_t^b \tag{8a}$$
$$MRisk_t^b \geq C_{ls} \cdot \underline{LR}_t^b \tag{8b}$$
$$MRisk_t^b \geq C_{rc} \cdot \overline{LR}_t^b \tag{8c}$$

where $MRisk_t^b$ considers the situation where all DR is failure and it takes bigger value of the increase of operation risk which is caused by uncertainty of DR. Since not all DR would fail at the same time, the increase of operation risk is assumed to a proportion α of $MRisk_t^b$. With the participation of DR in reducing the operation risk, the operation risk of load shedding and RE curtailment is $Risk_t^b + URisk_t^b$ after the consideration of uncertainty of DR, which is referred as the total operation risk of load shedding and RE curtailment in this paper.

3) Complete problem formulation: With the consideration of the operation risk, the complete problem formulation based on the proposed approach with the adjustable uncertainty set and the participation of DR is presented as,

$$\min_{\boldsymbol{u},\boldsymbol{v},\boldsymbol{y},\boldsymbol{x},\boldsymbol{a}} \Bigg\{ \sum_{t\in\mathcal{T}} \sum_{b\in\mathcal{B}} \sum_{i\in\mathcal{G}_b} SU_i^b u_{it}^b + SD_i^b v_{it}^b + F_i^b(y_{it}^b, x_{it}^b) + R_{ld}\underline{LR}_t^b + R_{li}\overline{LR}_t^b + \lambda \cdot (Risk_t^b + URisk_t^b) \Bigg\} \tag{9a}$$
$$s.t. (2b) - (2k), (4), (6), (7), (8) \tag{9b}$$

where $0 \leq \lambda \leq 1$ is the weight factor between both the operation cost of UC and the incentive payment for DR and the risk of load shedding and RE curtailment.

III. Solution Approach

Constraint (4) is nonlinear with (2b) introduced in it, and the nonlinearity of (4) makes (9) difficult to be solved directly. With (4) replaced by auxiliary variables and constraints, (9) is converted into a MILP problem. For constraint (4), the transformation of (4e) is illustrated as an example and the other constraints of (4) are transformed in a similar way. The steps of transformation are as follows,

Step1 Since constraint (4e) is linear with w_t^b, it is always satisfied if and only if it is satisfied at the bounds of the adjustable uncertainty set of RE, i.e., $w_t^b = LB'^b_t$ and $w_t^b = UB'^b_t$. The transformation of (4e) under the situation where $w_t^b = LB'^b_t$ is taken as an example and the transformations of (4e) under other situations are similar. Substituting (2b) and $w_t^b = LB'^b_t$ as shown in (3a) to (4e), (4e) is converted to

$$\sum_{b\in\mathcal{B}} K_l^b \Big(\sum_{r\in\mathcal{G}_b} (x_{rt}^b + a_{rt}^b \sum_{b\in\mathcal{B}} \underline{Q}_t^b \cdot \underline{\Delta}_t^b) - (\hat{\xi}_t^b - \hat{w}_t^b + \underline{Q}_t^b \cdot \underline{\Delta}_t^b) \Big) + C_l \geq 0. \tag{10}$$

Step2 A vector $Q_t^b = (\underline{q}_{t1}^b, \underline{q}_{t2}^b, \cdots, \underline{q}_{tn}^b, \cdots, \underline{q}_{tN}^b)^T$ is introduced with $\underline{q}_{t1}^b, \underline{q}_{t2}^b, \cdots, \underline{q}_{tn}^b, \cdots, \underline{q}_{tN}^b \in \{0, 1\}$. The integer variable $\underline{Q}_t^b$ with $0 \leq \underline{Q}_t^b \leq N$ is replaced by $\sum_{n=1}^N \underline{q}_{tn}^b$, and

TABLE I
ALL POSSIBLE PRODUCTS $h^b_{rtn} = a^b_{rt} \cdot \underline{q}^b_{tn}$

$\underline{q}^b_{tn}$	a^b_{rt}	$\underline{q}^b_{tn} \cdot a^b_{rt}$	constraints	imply
0	$0 \le a^b_{rt} \le 1$	0	$h^b_{rtn} \le 0$ $h^b_{rtn} \le a^b_{rt}$ $h^b_{rtn} \ge a^b_{rt} - 1$ $h^b_{rtn} \ge 0$	h^b_{rtn}=0
1	$0 \le a^b_{rt} \le 1$	a^b_{rt}	$h^b_{rtn} \le 1$ $h^b_{rtn} \le a^b_{rt}$ $h^b_{rtn} \ge a^b_{rt}$ $h^b_{rtn} \ge 0$	$h^b_{rtn} = a^b_{rt}$

(10) is equivalent to

$$\sum_{b\in\mathcal{B}} K^b_l \Big(\sum_{r\in\mathcal{G}_b} (x^b_{rt} + a^b_{rt} \sum_{b\in\mathcal{B}} (\sum_{n=1}^{N} \underline{q}^b_{tn}) \cdot \underline{\Delta}^b_t) - (\hat{\xi}^b_t - \hat{w}^b_t + (\sum_{n=1}^{N} \underline{q}^b_{tn}) \cdot \underline{\Delta}^b_t) \Big) + C_l \ge 0. \tag{11}$$

Step3 The product of a^b_{rt} and $\sum_{n=1}^{N} \underline{q}^b_{tn}$ is replaced by $\sum_{n=1}^{N} h^b_{rtn}$ with an auxiliary vector $H^b_{rt} = (h^b_{rt1}, h^b_{rt2}, \cdots, h^b_{rtn}, \cdots, h^b_{rtN})^T$ introduced, and (11) is equivalent to

$$\sum_{b\in\mathcal{B}} K^b_l \Big(\sum_{r\in\mathcal{G}_b} (x^b_{rt} + \sum_{b\in\mathcal{B}} (\sum_{n=1}^{N} h^b_{rtn}) \cdot \underline{\Delta}^b_t) - (\hat{\xi}^b_t - \hat{w}^b_t + (\sum_{n=1}^{N} \underline{q}^b_{tn}) \cdot \underline{\Delta}^b_t) \Big) + C_l \ge 0 \tag{12a}$$

$$H^b_{rt} \le Q^b_t \tag{12b}$$

$$H^b_{rt} \le a^b_{rt} \tag{12c}$$

$$H^b_{rt} \ge a^b_{rt} - (1 - Q^b_t) \tag{12d}$$

$$H^b_{rt} \ge 0. \tag{12e}$$

The equivalence of $a^b_{rt} \cdot \underline{q}^b_{tn}$ and h^b_{rtn} is ensured by constraints (12b)-(12e), and it is proved in Table I. After replacing $a^b_{rt} \cdot \underline{q}^b_{tn}$ with h^b_{rtn}, the UC problem based on the proposed approach is converted to be a MILP problem.

Discussion: Though bounds of the adjustable uncertainty set are determined not as continuous variables, the above solution approach transforms the problem to be linear and makes it to be solved by current solver through determining the adjustable uncertainty set among discrete subintervals of the maximum RE set.

IV. Simulation Results

This section presents the simulation results on the IEEE 6-bus, 30-bus and 300-bus systems to verify the effectiveness of the proposed approach. The details of 30-bus and 300-bus systems refer to Refs. [16] and [17], respectively, and those of the 6-bus system are given as follows. The diagram of the 6-bus system is presented in Fig. 3. There are two wind farms installed at bus 4 and bus 5, respectively, and the load at bus 4 and bus 5 can be adjusted as the source of DR to compensate

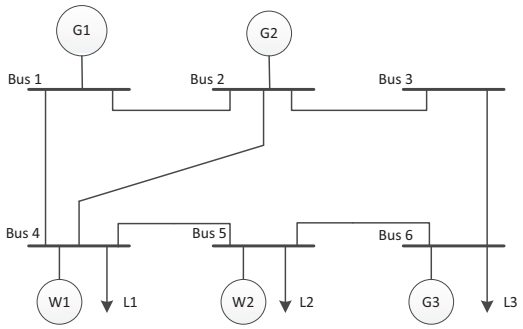

Fig. 3. Diagram of 6-bus test system

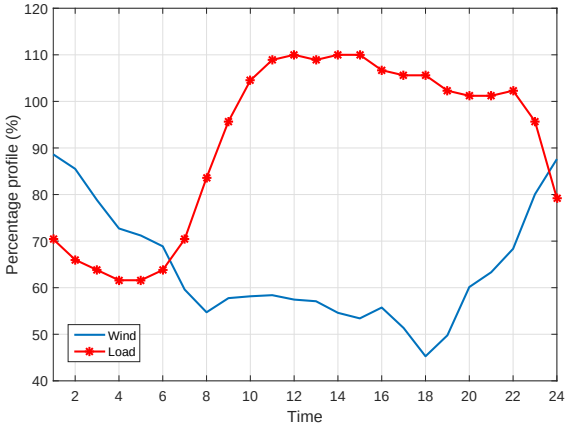

Fig. 4. Percentage profile of load and wind

the uncertainty of the wind generation. The network data of the 6-bus system is from MATPOWER 5.1 [18]. The detailed branch and load data are shown in Appendix. The unit data and the unit cost data shown in Appendix are from Ref. [19]. The initial states of the three units, G1-G3, are on, off and off, respectively, and the units have been in the initial states for the minimum up-time and down-time when they are to be scheduled. For all the loads in the 6-bus system, a load percentage profile in a day is assumed as shown in Fig. 4, and it shows the percentage between the load profile and the given load data in Appendix, i.e. the multiplication of the percentage and the load data indicates the load value. The capacities of two wind farms are assumed to be 30 MW and 10 MW, respectively, and Fig. 4 shows the forecast percentage profile of wind farms in a day which indicates the percentage between the forecast wind value and the capacity of a corresponding wind farm. The penalty prices of load shedding and wind curtailment are \$500/MWh and \$50/MWh [5], respectively. Incentive prices for load decrease and increase in DR are both \$1.1/MWh [14]. The proportion of DR failure, i.e., α is assumed to be 0.0001. All the simulations are programmed in MATLAB with YALMIP [20] as the modelling tool and Gurobi [21] as the MILP solver. The simulations run on a Win 10 PC with a 3.2 GHz CPU and 32 GB RAM. The successive constraint enforcement scheme for the line flow limits [22] is employed in 30-bus and 300-bus systems to

improve computational efficiency.

The proposed approach is investigated from the following three aspects: (i) comparisons between the proposed approach and the ROA together with a method that constrains the deviation from the forecast RE; (ii) the comparison between situations with and without DR; (iii) the sensitivities of parameters of the proposed approach. Firstly, the above three aspects of the proposed approach on the 6-bus system are presented in three subsections. Then, the effectiveness of the proposed approach is further tested on 30-bus and 300-bus systems in the fourth subsection. The method that constrains the deviation from the forecast RE is referred to CROA for convenience. The CROA is formulated as (9) together with the following constraints which limit the deviation from the forecast,

$$\sum_{t=1}^{T} \underline{Q}_t^b \geq \underline{\gamma}^b \tag{13a}$$

$$\sum_{t=1}^{T} \overline{Q}_t^b \geq \overline{\gamma}^b \tag{13b}$$

where they indicate the negative and positive deviation numbers of wind farm at bus b in the scheduling horizon should be greater than $\underline{\gamma}^b$ and $\overline{\gamma}^b$, respectively. Compared with the CROA, the proposed approach does not require the constraints to confine the deviation from the forecast RE.

A. The comparison between the proposed approach and other methods

With $LB_t^4 = 0$, $UB_t^4 = 30$ MW, $LB_t^5 = 0$ and $UB_t^5 = 10$ MW $\forall t \in \mathcal{T}$, the proposed approach under the situation where $N = 25, \lambda = 0.2, \underline{LR}_{\max}^4 = \overline{LR}_{\max}^4 = \underline{LR}_{\max}^5 = \overline{LR}_{\max}^5 = 3$ MW, $\beta_4 = \beta_5 = 18$ MWh is compared with the ROA and CROA with $\underline{\gamma}^4 = \overline{\gamma}^4 = \underline{\gamma}^5 = \overline{\gamma}^5 = 576$. Table II shows the solution of UC of the proposed approach. The two figures in Fig. 5 show the adjustable uncertainty sets of the two wind farms, i.e., LB'^4_t and UB'^4_t, and LB'^5_t and UB'^5_t, respectively. Fig. 6 shows DR at bus 4 and bus 5, respectively. The situation at each time slot in Fig. 5 is a specialization of Fig. 2. For example, the points (5.58,10) and (17.45,10) represent the lower and upper bounds of the adjustable uncertainty set of RE are 5.58 MW and 17.45 MW at time slot 10, respectively. Similar as Fig. 2, the gap between the lower bound of the maximum RE set (0,10) and blue star (3,10) is 3 MW, and the gap between red triangle (30,10) and the upper bound of the maximum RE set (30,10) is 0, which represent the load decrease and load increase in DR, respectively. Black line between blue star and (5.58,10) and black line between (17.45,10) and red triangle represent the risk of load shedding and the risk of RE curtailment, respectively. It can be seen from Fig. 5 that the adjustable uncertainty set of the proposed approach is the subset of the maximum uncertainty set of the ROA, which makes the proposed approach less conservative. Fig. 5 also shows DR helps reduce the risk of load shedding and RE curtailment.

Table III shows the performance of the proposed approach, the ROA and the CROA, including the value of the objective function, i.e., (9a), the operation cost of UC, i.e.,

TABLE II
UC SOLUTION OF 6-BUS SYSTEM BASED ON THE PROPOSED APPROACH

Time	Generator 1		Generator 2		Generator 3	
	x_1 (100MW)	a_1	x_2 (100MW)	a_2	x_3 (100MW)	a_3
1	1.617	1.000	off	0.000	off	0.000
2	1.506	1.000	off	0.000	off	0.000
3	1.471	1.000	off	0.000	off	0.000
4	1.434	1.000	off	0.000	off	0.000
5	1.440	1.000	off	0.000	off	0.000
6	1.511	1.000	off	0.000	off	0.000
7	1.733	1.000	off	0.000	off	0.000
8	1.824	1.000	off	0.000	0.298	0.000
9	1.950	0.999	off	0.000	0.498	0.000
10	2.142	0.000	off	0.000	0.552	1.000
11	1.650	0.425	0.568	0.137	0.598	0.438
12	1.507	0.685	0.704	0.000	0.639	0.315
13	1.406	0.685	0.779	0.000	0.636	0.315
14	1.494	0.685	0.720	0.000	0.647	0.315
15	1.531	0.685	0.693	0.000	0.642	0.315
16	1.220	0.682	0.915	0.002	0.630	0.315
17	1.182	0.373	0.947	0.258	0.622	0.368
18	1.622	0.223	0.563	0.206	0.592	0.571
19	2.060	0.449	off	0.000	0.606	0.551
20	2.015	0.498	off	0.000	0.578	0.502
21	2.010	0.497	off	0.000	0.571	0.504
22	2.027	0.449	off	0.000	0.564	0.551
23	1.863	1.000	off	0.000	0.497	0.000
24	1.570	1.000	off	0.000	0.297	0.000

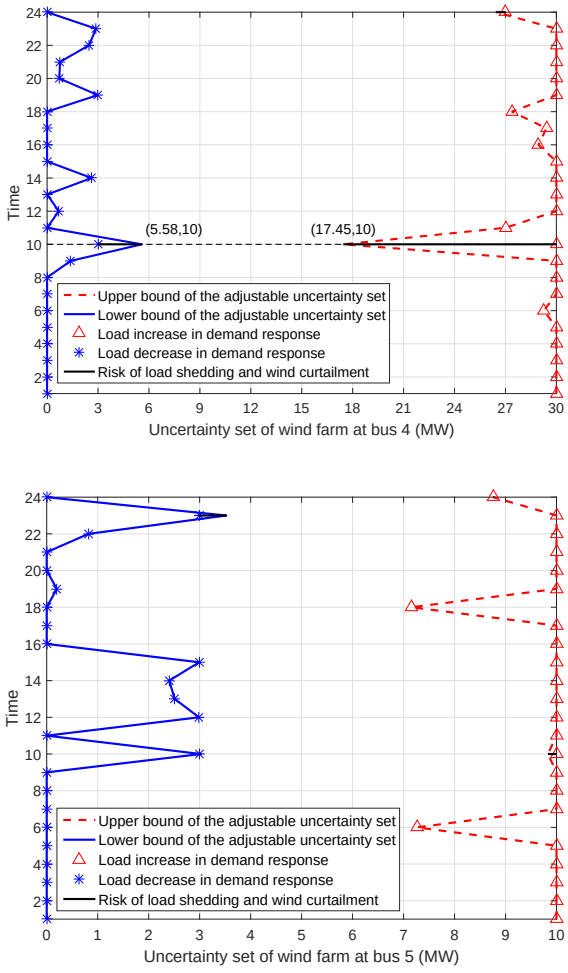

Fig. 5. Adjustable uncertainty sets of wind farms at bus 4 and bus 5

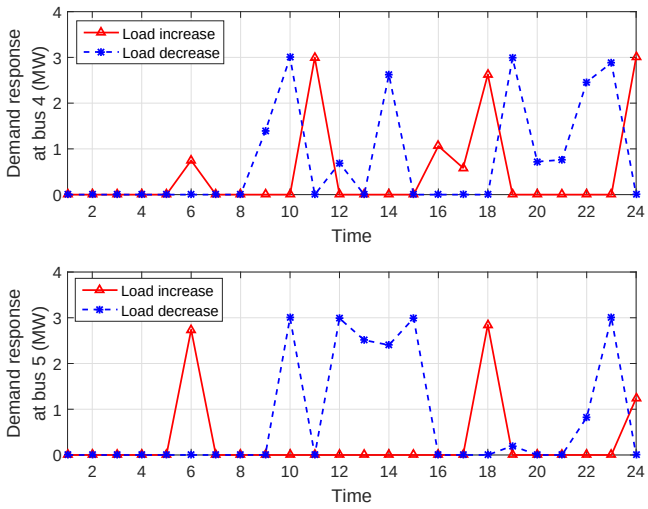

Fig. 6. Demand response at bus 4 and bus 5

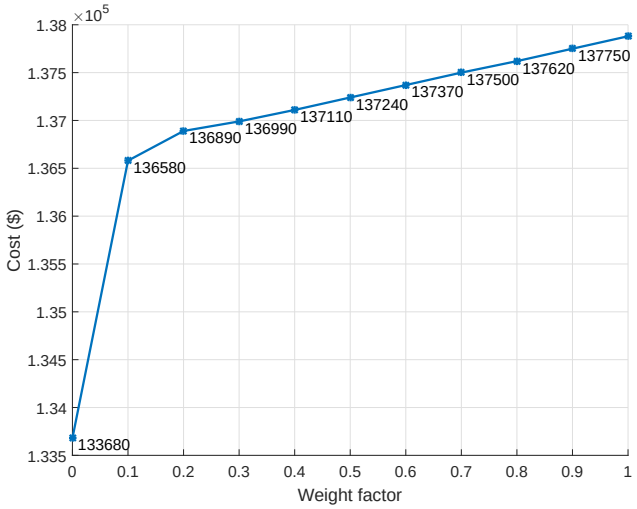

Fig. 7. Sensibility of the weight factor

TABLE III
COMPARISON AMONG PROPOSED APPROACH, CROA AND ROA ON 6-BUS SYSTEM

	Proposed approach	CROA	ROA
Objective function (10^5 \$)	1.365	1.367	1.391
Operation cost of UC (10^5 \$)	1.361	1.366	1.391
Operation risk (\$)	1604.645	443.890	0

$\sum_{t\in\mathcal{T}}\sum_{b\in\mathcal{B}}\sum_{i\in\mathcal{G}_b} SU_i^b u_{it}^b + SD_i^b v_{it}^b + F_i^b(y_{it}^b, x_{it}^b)$, and the total operation risk of load shedding and RE curtailment, i.e., $\sum_{t\in\mathcal{T}}\sum_{b\in\mathcal{B}} Risk_t^b + URisk_t^b$. Compared with the the CROA and ROA, the proposed approach helps reduce the value of objective function and the operation cost of UC. Since DR is not taken into account in ROA, the situation of the proposed approach is compared with ROA that DR is not considered with $\underline{LR}^4_{\max} = \overline{LR}^4_{\max} = \underline{LR}^5_{\max} = \overline{LR}^5_{\max} = 0$ MW, $\beta_4 = \beta_5 = 0$ MWh and that the operation risk is taken into account with $\lambda = 1$. The values of the objective function of the proposed approach and ROA are $\$1.386 \times 10^5$ and $\$1.391 \times 10^5$, respectively, and the value of the proposed approach is reduced in comparison with ROA.

To test the proposed approach, 10000 scenarios of two wind farms are generated based on Beta distribution [23]. Gumbel copulas is introduced to model the dependence of these two wind farms [24]. The normalized expectation of wind power output is from Fig. 4, the hour-to-hour standard deviation is set to be 0.05 and the rank correlation is set to be 0.05. The average costs of the proposed approach, CROA and ROA including the operation cost of UC, the compensation cost for DR and the cost of load shedding and RE curtailment are $\$1.352 \times 10^5$, $\$1.357 \times 10^5$ and $\$1.381 \times 10^5$, respectively. The cost of the proposed approach is the smallest.

B. The comparison between situations with and without demand response

With $LB_t^4 = 0$, $UB_t^4 = 30$ MW, $LB_t^5 = 0$ and $UB_t^5 = 10$ MW $\forall t \in \mathcal{T}$, $N = 25$ and $\lambda = 0.2$, the proposed approach with $\underline{LR}^4_{\max} = \underline{LR}^5_{\max} = \overline{LR}^4_{\max} = \overline{LR}^5_{\max} = 3$ MW, $\beta_4 = \beta_5 = 18$ MWh is compared with that without DR, i.e., $\underline{LR}^4_{\max} = \underline{LR}^5_{\max} = \overline{LR}^4_{\max} = \overline{LR}^5_{\max} = \beta_4 = \beta_5 = 0$. The values of the objective function for situations with and without DR are $\$1.365 \times 10^5$ and $\$1.382 \times 10^5$, respectively. The proposed approach with the participation of DR reduces the value of the objective function in comparison with the situation without DR.

As shown in Fig. 5, the proposed approach with the participation of DR mitigates the risk of load shedding and wind curtailment. When the adjustable uncertainty sets as shown in Fig. 5 are adopted, the cost of load shedding and wind curtailment is \$20195.221 without DR, while the cost of the total risk is \$1604.645 with DR. The cost of risk is reduced by \$18590.576 through the participation of DR. DR helps greatly in reducing the risk of load shedding and wind curtailment.

C. Sensitivities of parameters of the proposed approach

In this subsection, sensitivities of parameters of the proposed approach, including the division number N, the weight factor λ, and the capacity of DR with $\underline{LR}^b_{\max}$, $\overline{LR}^b_{\max}$ and β_b are investigated. With $N = 25, \underline{LR}^4_{\max} = \overline{LR}^4_{\max} = \underline{LR}^5_{\max} = \overline{LR}^5_{\max} = 2$ MW and $\beta_4 = \beta_5 = 12$ MWh, Fig. 7 shows the sensibility of λ. It can be seen from Fig. 7 that with the increase of the weight factor, the cost of the objective function increases. With $N = 25, \lambda = 0.2$, and $\underline{LR}^4_{\max} = \overline{LR}^4_{\max} = \underline{LR}^5_{\max} = \overline{LR}^5_{\max} = 0.3$ MW and $\beta_4 = \beta_5 = 1.8$ MWh as a unit of the capacity of DR, Fig. 8 shows the sensibility of the capacity of DR. The situation where the capacity of DR is 5 in Fig. 8 indicates $\underline{LR}^4_{\max} = \overline{LR}^4_{\max} = \underline{LR}^5_{\max} = \overline{LR}^5_{\max} = 1.5$ MW and $\beta_4 = \beta_5 = 9$ MWh. It can be seen from Fig. 8 that with the increase of the capacity of DR, the cost of objective function decreases.

With $\lambda = 0.2, \underline{LR}^4_{\max} = \overline{LR}^4_{\max} = \underline{LR}^5_{\max} = \overline{LR}^5_{\max} = 2$ MW and $\beta_4 = \beta_5 = 12$ MWh, Fig. 9 shows the sensibility of N. When the division number is 0, the intercept of vertical axis indicates the cost of the ROA in Fig. 9. It can be seen

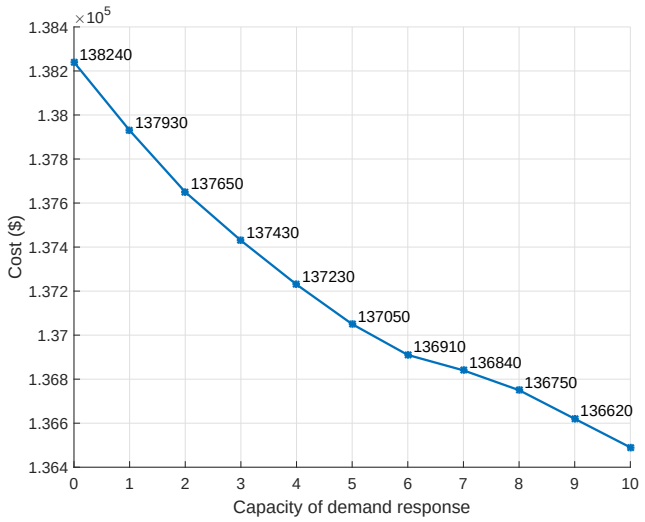

Fig. 8. Sensibility of the capacity of demand response

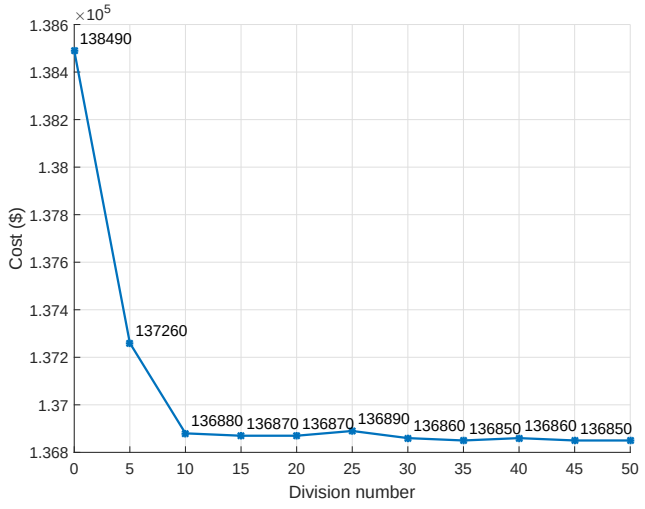

Fig. 9. Sensibility of the division number

from Fig. 9 that with the increase of the division number, the cost of objective function decreases but not monotonously. Due to that the proposed approach is to determine the bounds of the adjustable uncertainty set through dividing the maximum uncertainty set and that the division is discrete, the decrease of the cost is not monotonous, which is illustrated through Fig. 10. The feasible sets of the lower bound of the adjustable uncertainty set under the situations where $N = 2, 3$ and 4 are $\{LB_t^b, A, \hat{w_t^b}\}$, $\{LB_t^b, B, C, \hat{w_t^b}\}$ and $\{LB_t^b, D, A, E, \hat{w_t^b}\}$, respectively. The feasible sets of the upper bound of the adjustable uncertainty set are similar. The feasible set under the situation where $N = 2$ is the subset of that of the situation where $N = 4$, i.e., the number of feasible solutions for $N = 4$ is larger than that for $N = 2$. Therefore, the cost of objective function decreases when N increases from 2 to 4. However, it is not the case for the situations where $N = 2$ and $N = 3$ when their feasible sets of the bounds of the adjustable uncertainty set are compared. Therefore, the cost of the objective function may not decrease when N increases from 2 to 3.

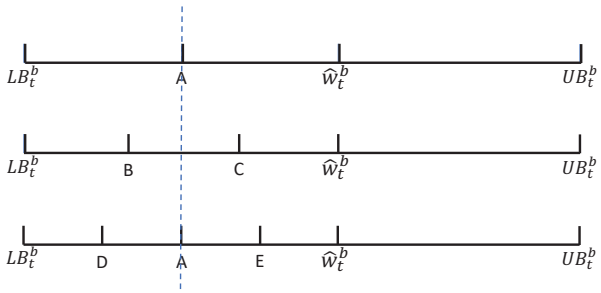

Fig. 10. Feasible sets of the lower bound of the adjustable uncertainty set under the situations where $N = 2, 3$ and 4

TABLE IV
COMPARISON OF VALUE OF OBJECTIVE FUNCTION AMONG PROPOSED APPROACH, CROA AND ROA ON 30-BUS AND 300-BUS SYSTEMS

Objective value	Proposed approach	CROA	ROA
30-bus system (10^5 \$)	1.352	1.357	1.362
300-bus system (10^6 \$)	8.840	8.845	8.847

D. Verification on 30-bus and 300-bus systems

In order to further test the proposed approach of an adjustable uncertainty set together with DR for the reduction of load shedding and RE curtailment, the IEEE 30-bus system with two wind farms installed and 300-bus system with two wind farms installed are adopted as test systems. The details of 30-bus and 300-bus systems refer to Refs. [16] and [17], respectively. Both capacities of wind farms of 30-bus system are assumed to be 20 MW and they are 300 MW for 300-bus system. The loads at buses where wind farms are installed can be adjusted as DR sources to compensate the uncertainty of the wind generation.

To verify the effectiveness of the adjustable uncertainty set, the proposed approach with $N = 5, \lambda = 0.2$ and without DR is compared with ROA and CROA with positive and negative deviation number greater than 118 on 30-bus and 300-bus systems. Table IV shows the comparison among the proposed approach, the CROA and the ROA on 30-bus and 300-bus systems. For 30-bus system, the values of objective function are $\$1.352 \times 10^5$, $\$1.357 \times 10^5$ and $\$1.362 \times 10^5$ for the proposed approach, CROA and ROA, respectively. For 300-bus system, they are $\$8.840 \times 10^6$, $\$8.845 \times 10^6$ and $\$8.847 \times 10^6$, respectively. The proposed approach with adjustable uncertainty set reduces the value of objective function in comparison with CROA and ROA. To make the comparison between the proposed approach and ROA more clear, the situation of the proposed approach is compared with ROA that DR is not considered and that the operation risk is taken into account with $\lambda = 1$. For 30-bus system, the values of objective function are $\$1.358 \times 10^5$ and $\$1.362 \times 10^5$ for the proposed approach and ROA, respectively. For 300-bus system, they are $\$8.845 \times 10^6$ and $\$8.847 \times 10^6$, respectively.

With $N = 5$ and $\lambda = 0.2$, the proposed approach with the participation of DR is compared with the situation without DR on 30-bus and 300-bus systems. For 30-bus system, $\underline{LR}_{\max} = \overline{LR}_{\max} = 2$ MW and $\beta = 12$ MWh for both DR at two buses where wind farms are installed. It is $\underline{LR}_{\max} = \overline{LR}_{\max} = 40$ MW and $\beta = 500$ MWh for 300-bus system. The UC

TABLE V
COMPARISON VALUE OF OBJECTIVE FUNCTION BETWEEN SITUATIONS WITH AND WITHOUT DR ON 30-BUS AND 300-BUS SYSTEMS

Objective value	With DR	Without DR
30-bus system (10^5 \$)	1.338	1.352
300-bus system (10^6 \$)	8.833	8.840

solution of 30-bus system of the proposed approach with DR is presented in Appendix and that of 300-bus system refers to [25]. Table V shows the comparison between situations with and without DR on 30-bus and 300-bus systems. For 30-bus system, the values of objective function are $\$1.338 \times 10^5$ and $\$1.352 \times 10^5$ for the situations with and without DR, respectively. For 300-bus system, they are $\$8.833 \times 10^6$ and $\$8.840 \times 10^6$, respectively. The proposed approach with the participation of DR reduces the value of objective function in comparison with the situation without DR. The computation time of the proposed approach with DR is 2253.8 seconds for the 300-bus system, which shows the feasibility of the proposed approach in reality.

V. CONCLUSION

In this paper, the approach of an adjustable uncertainty set is proposed to schedule UC with the consideration of the uncertainty of RE, and DR is utilized in reducing the operation risk of load shedding and RE curtailment when the RE falls out of the adjustable uncertainty set. The proposed approach divides the maximum uncertainty set of RE into subintervals and determines bounds of the adjustable uncertainty set among these subintervals without the deviation constraints of RE from the forecast. Simulation results have demonstrated that the proposed approach reduces the cost of system operation of UC in comparison with ROA and CROA, and the operation risk is reduced with the participation of DR. A larger capacity of DR will bring more benefit to the operation of UC. Future work will focus on the achievement of DR in detail and the combination of the proposed approach and the detailed achievement of DR will also be studied.

APPENDIX

TABLE VI
LOAD DATA OF 6-BUS SYSTEM

Load 1 (MW)	Load 2 (MW)	Load 3 (MW)
56	112	112

TABLE VII
BRANCH DATA OF 6-BUS SYSTEM

fbus	tbus	resistance (p.u.)	reactance (p.u.)	susceptance (p.u.)	limit (MVA)
1	2	0.10	0.170	0.04	200
2	3	0.05	0.037	0.04	100
1	4	0.08	0.258	0.06	100
2	4	0.05	0.197	0.06	100
4	5	0.05	0.037	0.02	100
5	6	0.10	0.140	0.04	100
3	6	0.07	0.018	0.05	100

TABLE VIII
UNIT DATA OF 6-BUS SYSTEM

	L (MW)	U (MW)	UR (MW)	DR (MW)
Unit1	100	220	55	55
Unit2	10	100	50	50
Unit3	10	70	20	20
	$\overline{UR}$ (MW)	$\overline{DR}$ (MW)	MU (h)	MD (h)
Unit1	100	100	4	4
Unit2	60	60	3	2
Unit3	30	30	1	1
	SU(\$)	SD(\$)	f_0^1(\$)	f_1^1 (\$/MW)
Unit1	900	450	394.280	20.655
Unit2	550	275	699.200	16.700
Unit3	170	85	367.864	22.545
	f_0^2(\$)	f_1^2 (\$/MW)	f_0^3(\$)	f_1^3 (\$/MW)
Unit1	349.704	20.974	292.392	21.292
Unit2	694.400	16.820	686.000	16.940
Unit3	359.320	22.830	345.080	23.114

TABLE IX
UC SOLUTION OF 30-BUS SYSTEM BASED ON THE PROPOSED APPROACH

Time	Generator at bus 1		Generator at bus 2		Generator at bus 13	
	x (100MW)	a	x (100MW)	a	x (100MW)	a
1	0.336	0.000	0.380	1.000	0.100	0.000
2	0.600	0.128	0.437	0.873	off	0.000
3	0.565	0.118	0.453	0.882	off	0.000
4	0.495	1.000	0.500	0.000	off	0.000
5	0.471	0.000	0.529	1.000	off	0.000
6	0.491	1.000	0.564	0.000	off	0.000
7	0.600	0.234	0.627	0.766	off	0.000
8	0.689	0.266	0.641	0.734	off	0.000
9	0.690	0.822	0.800	0.000	off	0.000
10	0.639	0.727	0.800	0.000	off	0.000
11	0.800	0.000	0.680	0.543	off	0.000
12	0.800	0.000	0.674	0.578	off	0.000
13	0.800	0.000	0.688	0.518	off	0.000
14	0.800	0.000	0.706	0.455	off	0.000
15	0.800	0.000	0.689	0.602	off	0.000
16	0.668	0.622	0.800	0.000	off	0.000
17	0.691	0.557	0.800	0.000	off	0.000
18	0.713	0.631	0.800	0.000	off	0.000
19	0.666	0.789	0.786	0.083	off	0.000
20	0.800	0.000	0.640	0.876	off	0.000
21	0.800	0.000	0.633	0.869	off	0.000
22	0.781	0.073	0.605	0.750	off	0.000
23	0.606	0.640	0.800	0.000	off	0.000
24	0.505	0.163	0.521	0.837	off	0.000
Time	Generator at bus 22		Generator at bus 23		Generator at bus 27	
	x (100MW)	a	x (100MW)	a	x (100MW)	a
1	0.100	0.000	0.100	0.000	0.100	0.000
2	off	0.000	off	0.000	off	0.000
3	off	0.000	off	0.000	off	0.000
4	off	0.000	off	0.000	off	0.000
5	off	0.000	off	0.000	off	0.000
6	off	0.000	off	0.000	off	0.000
7	off	0.000	off	0.000	off	0.000
8	0.190	0.000	off	0.000	off	0.000
9	0.266	0.178	off	0.000	off	0.000
10	0.297	0.273	off	0.000	0.200	0.000
11	0.292	0.249	off	0.000	0.254	0.207
12	0.292	0.246	off	0.000	0.286	0.176
13	0.273	0.182	off	0.000	0.270	0.300
14	0.268	0.364	off	0.000	0.289	0.181
15	0.280	0.176	off	0.000	0.298	0.222
16	0.275	0.332	off	0.000	0.247	0.046
17	0.280	0.168	off	0.000	0.214	0.275
18	0.307	0.279	off	0.000	0.188	0.090
19	0.343	0.000	off	0.000	0.127	0.128
20	0.420	0.124	off	0.000	off	0.000
21	0.415	0.131	off	0.000	off	0.000
22	0.341	0.000	off	0.000	0.125	0.177
23	0.265	0.361	off	0.000	off	0.000
24	0.275	0.000	off	0.000	off	0.000

REFERENCES

[1] FS-UNEP collaborating center, Global trends in renewable energy investment 2016 [Online]. Available: http://fs-unep-centre.org/sites/default/files/publications/globaltrendsinrenewableenergyinvestment2016lowres_0.pdf.

[2] A. Nikoobakht, J. Aghaei, T. Niknam, V. Vahidinasab, H. Farahmand, and M. Korpas, "Towards robust OPF solution strategy for the future AC/DC grids: case of VSC-HVDC-connected offshore wind farms," *IET Renewable Power Generation*, vol. 12, no. 6, pp. 691–701, 2018.

[3] M. Alipour, B. Mohammadi-Ivatloo, and K. Zare, "Stochastic scheduling of renewable and CHP-based microgrids," *IEEE Transactions on Industrial Informatics*, vol. 11, no. 5, pp. 1049–1058, Oct. 2015.

[4] L. Zhao and B. Zeng, "Robust unit commitment problem with demand response and wind energy," in *2012 IEEE Power and Energy Society General Meeting*, July 2012, pp. 1–8.

[5] C. Duan, L. Jiang, W. Fang, and J. Liu, "Data-driven affinely adjustable distributionally robust unit commitment," *IEEE Transactions on Power Systems*, vol. 33, no. 2, pp. 1385–1398, Mar. 2018.

[6] C. Wang, F. Liu, J. Wang, W. Wei, and S. Mei, "Risk-based admissibility assessment of wind generation integrated into a bulk power system," *IEEE Transactions on Sustainable Energy*, vol. 7, no. 1, pp. 325–336, Jan. 2016.

[7] C. Wang, F. Liu, J. Wang, F. Qiu, W. Wei, S. Mei, and S. Lei, "Robust risk-constrained unit commitment with large-scale wind generation: An adjustable uncertainty set approach," *IEEE Transactions on Power Systems*, vol. 32, no. 1, pp. 723–733, Jan. 2017.

[8] C. Dai, L. Wu, and H. Wu, "A multi-band uncertainty set based robust SCUC with spatial and temporal budget constraints," *IEEE Transactions on Power Systems*, vol. 31, no. 6, pp. 4988–5000, Nov. 2016.

[9] W. A. Bukhsh, C. Zhang, and P. Pinson, "An integrated multiperiod OPF model with demand response and renewable generation uncertainty," *IEEE Transactions on Smart Grid*, vol. 7, no. 3, pp. 1495–1503, May 2016.

[10] W. Li, P. Du, and N. Lu, "Design of a new primary frequency control market for hosting frequency response reserve offers from both generators and loads," *IEEE Transactions on Smart Grid*, vol. 9, no. 5, pp. 4883–4892, Sep. 2018.

[11] R. A. Jabr, "Adjustable robust OPF with renewable energy sources," *IEEE Transactions on Power Systems*, vol. 28, no. 4, pp. 4742–4751, Nov. 2013.

[12] N. Lu and Y. Zhang, "Design considerations of a centralized load controller using thermostatically controlled appliances for continuous regulation reserves," *IEEE Transactions on Smart Grid*, vol. 4, no. 2, pp. 914–921, June 2013.

[13] H. Wu, M. Shahidehpour, A. Alabdulwahab, and A. Abusorrah, "Thermal generation flexibility with ramping costs and hourly demand response in stochastic security-constrained scheduling of variable energy sources," *IEEE Transactions on Power Systems*, vol. 30, no. 6, pp. 2955–2964, Nov. 2015.

[14] M. Vrakopoulou, J. L. Mathieu, and G. Andersson, "Stochastic optimal power flow with uncertain reserves from demand response," in *2014 47th Hawaii International Conference on System Sciences*, Jan. 2014, pp. 2353–2362.

[15] Y. Zhang, S. Shen, and J. L. Mathieu, "Distributionally robust chance-constrained optimal power flow with uncertain renewables and uncertain reserves provided by loads," *IEEE Transactions on Power Systems*, vol. 32, no. 2, pp. 1378–1388, Mar. 2017.

[16] Y. F. Du, Data of 30-bus system [Online]. Available: https://www.researchgate.net/publication/336412671_Data_of_30-bus_system.

[17] Y. F. Du, Data of 300-bus system [Online]. Available: https://www.researchgate.net/publication/336412564_Data_of_300-bus_system.

[18] MATPOWER, Free, open-source Electric Power System Simulation and Optimization Tools for MATLAB and Octave [Online]. Available: http://www.pserc.cornell.edu/matpower/.

[19] A. L. Diniz, "Test cases for unit commitment and hydrothermal scheduling problems," in *IEEE PES General Meeting*, July 2010, pp. 1–8.

[20] J. Lofberg, "Yalmip : a toolbox for modeling and optimization in matlab," in *2004 IEEE International Symposium on Computer Aided Control Systems Design*, Sep. 2004, pp. 284–289.

[21] Gurobi Optimization Incorporated, *Gurobi optimizer reference manual*, 2015.

[22] R. A. Jabr, S. Karaki, and J. A. Korbane, "Robust multi-period OPF with storage and renewables," *IEEE Transactions on Power Systems*, vol. 30, no. 5, pp. 2790–2799, Sep. 2015.

[23] H. Louie and J. Sloughter, "Probabilistic modeling and statistical characteristics of aggregate wind power," *Green Energy and Technology*, pp. 19–51, 01 2014.

[24] H. Louie, "Evaluation of bivariate Archimedean and elliptical copulas to model wind power dependency structures," *Wind Energy*, vol. 17, no. 2, pp. 225–240, 2014.

[25] Y. F. Du, Unit commitment solution of 300-bus system [Online]. Available: https://www.researchgate.net/publication/336412581_UCSolutionof300bus.

Y. F. Du (M'19) received the B.Eng. degree from the University of Electronic Science and Technology of China, Chengdu, China, in 2013, and the Ph.D. degree from the University of Liverpool, U.K., in 2017, both in electrical engineering. She worked as a postdoctoral research fellow in Nanyang Technological University, Singapore, in 2018. Currently, she is a lecturer in the University of Electronic Science and Technology of China. Her research interests include demand response in smart grid, optimal power system scheduling and renewable energy.

Y. Z. Li (M'18) received the M.S. degree and Ph.D. degree in electrical engineering from the Huazhong University of Science and Technology, Wuhan, China, and the South China University of Technology, Guangzhou, China, in 2011 and 2015, respectively. He has published several peer-reviewed papers in international journals. His current research interests include optimal power system/microgrid scheduling and decisionmaking, stochastic optimization considering large-scale integration of renewable energy into the power system and multiobjective optimization.

C. Duan (S'14-M'19) received a B.S. degree from Xi'an Jiaotong University, Xi'an, China, in 2012, and dual Ph.D. degrees from Xi'an Jiaotong University and the University of Liverpool, U.K. in 2018, all in electrical engineering. He has been a postdoctoral fellow and then a research assistant professor with the Department of Physics and Astronomy, Northwestern University, Evanston, U.S. since 2018. His research interests include power system operation, network dynamics, and system control.

H. B. Gooi (SM'95) received the B.S. degree in electrical engineering from National Taiwan University, Taipei, Taiwan, in 1978; the M.S. degree in power engineering from the University of New Brunswick, Fredericton, NB, Canada, in 1980; and the Ph.D. degree in power engineering from the Ohio State University, Columbus, OH, USA, in 1983.

From 1983 to 1985, he was an Assistant Professor with the Department of Electrical Engineering, Lafayette College, Easton, PA, USA. From 1985 to 1991, he was a Senior Engineer with Empros (now Siemens), Minneapolis, MN, USA, where he was responsible for the design and testing coordination of domestic and international energy management system projects. In 1991, he joined the School of Electrical and Electronic Engineering, Nanyang Technological University, Singapore, as a Senior Lecturer, where he has been an Associate Professor since 1999 and the Deputy Head of Power Engineering Division from 2008 to 2014. Starting 2020, he serves as a Co-Director of Singapore Power-NTU Joint Lab. He has served as Associate Editor, IEEE Transactions on Power Systems since 2016. His current research interests include microgrid energy management systems, electricity markets, spinning reserve, energy storage, and renewable energy sources.

L Jiang (M'00) received the B.S. and M.S. degrees from Huazhong University of Science and Technology (HUST), China, in 1992 and 1996; and the Ph.D. degree from the University of Liverpool, UK, in 2001, all in Electrical Engineering. He worked as a Postdoctoral Research Assistant in the University of Liverpool from 2001 to 2003, and Postdoctoral Research Associate in the Department of Automatic Control an Systems Engineering, the University of Sheffield from 2003 to 2005. He was a Senior Lecturer at the University of Glamorgam from 2005 to 2007 and moved to the University of Liverpool in 2007. Currently, he is a Reader in The University of Liverpool. His current research interests include control and analysis of power system, smart grid, and renewable energy.